ISSN 1063-7729, Astronomy Reports, 2015, Vol. 59, No. 9, pp. 879–887. © Pleiades Publishing, Ltd., 2015.
Original Russian Text © I.S. Savanov, E.S. Dmitrienko, 2015, published in Astronomicheskii Zhurnal, 2015, Vol. 92, No. 9, pp. 758–766.

Activity and Cool Spots on the Surfaces of G-type Stars with Superflares from Observations with the Kepler Space Telescope

I. S. Savanov[1]* and E. S. Dmitrienko[2]

[1]*Institute of Astronomy, Russian Academy of Sciences, Pyatnitskaya 48, Moscow, 119017 Russia*

[2]*Sternberg Astronomical Institute, Lomonosov Moscow Moscow State University, Universitetskii pr. 13, Moscow, 119992 Russia*

Received March 11, 2015; in final form, April 10, 2015

Abstract—The properties of active regions (cool spots) on the surfaces of 279 G-type stars in which more than 1500 superflares with energies of 10^{33}–10^{36} erg were detected are analyzed. Diagrams plotting the superflare energy against activity parameters of the stars (the area of their magnetic spots) are considered, and a more extensive study of the activity of two stars with the highest numbers of flares is presented. The range of variation of the superflare energies (up to two orders of magnitude) is realized over the entire interval of rotation periods. It is proposed that the plot of superflare energy vs. rotational period is bimodal. There are probably no appreciable differences in the maximum flare energies for the two groups of objects, which have rotational periods of more than and less than 10 days. Three groups of stars with different surface spottednesses can be distinguished in a plot of superflare energy vs. cool-spot area. The range of variation of the flare energy within a group is roughly the same for these three groups. Most of the points on this diagram lie to the right of the dependence corresponding to $B = 3000$ G and an inclination $i = 90°$ (the first two groups of objects). It is confirmed that the flare activity is not related directly to circumpolar active regions, since the majority of the points on the diagram lie to the right of the dependence for $B = 1000$ G and $i = 3°$. Analysis of stars from the sample, including objects with more than 20 superflares, shows that large variations of the energy (by up to two orders of magnitude) can be reached with small variations of the spottedness parameter S for a single star. Appreciable variability of the spottedness (by factors of five to six) was detected for only two objects from the sample (KIC 10422252 and KIC 11764567). These stars displayed an increase in the flare energy by orders of magnitude for any spottedness level. The activity of KIC 11551430 and KIC 11764567 is analyzed in detail using all available photometric data from the Kepler Space Telescope archives. KIC 11551430 was determined earlier to display the highest number of flares (on average, one flare every 7 days); KIC 11764567 displayed the highest number of flares among stars with rotational periods comparable to the solar period (on average, one flare every 25 days). Maps of surface temperature inhomogeneities of these stars are used to determine the longitudes and other characteristics of their active regions.

DOI: 10.1134/S1063772915090073

1. INTRODUCTION

Their analysis of extensive photometric data obtained with the Kepler Space Telescope enabled Maehara et al. [1] to discover a large number of high-energy superflares of solar-type stars, opening the way to statistical analyses of this phenomenon. The energies of the detected superflares appreciably exceed 10^{33} erg, and their durations are several hours. For comparison, the energy of the Carrington event of September 1, 1859 is estimated to be $\geq 10^{32}$ erg [2]. It is very striking that one encounters slowly rotating stars (with periods of more than 10 days) among solar-type stars with superflares. This raises the question: is the Sun capable of generating flares with such energies, and do stars with superflares possess some characteristics distinguishing them from the Sun?

The main conclusion of our study [3] (based on the observational data of [4]) is the enhanced spottedness of the surfaces of stars with superflares, which testifies to enhanced magnetic activity on these stars. Analysis of the data of [5] enabled us to confirm the enhanced spottedness of the surfaces of stars displaying superflares based on an independent treatment of the brightness variability. These same data [5] testify that, in spite of their enhanced spottedness, stars with superflares are not distinguishable from the overall set of stars in terms of the parameter of their differential

*E-mail: isavanov@inasan.ru

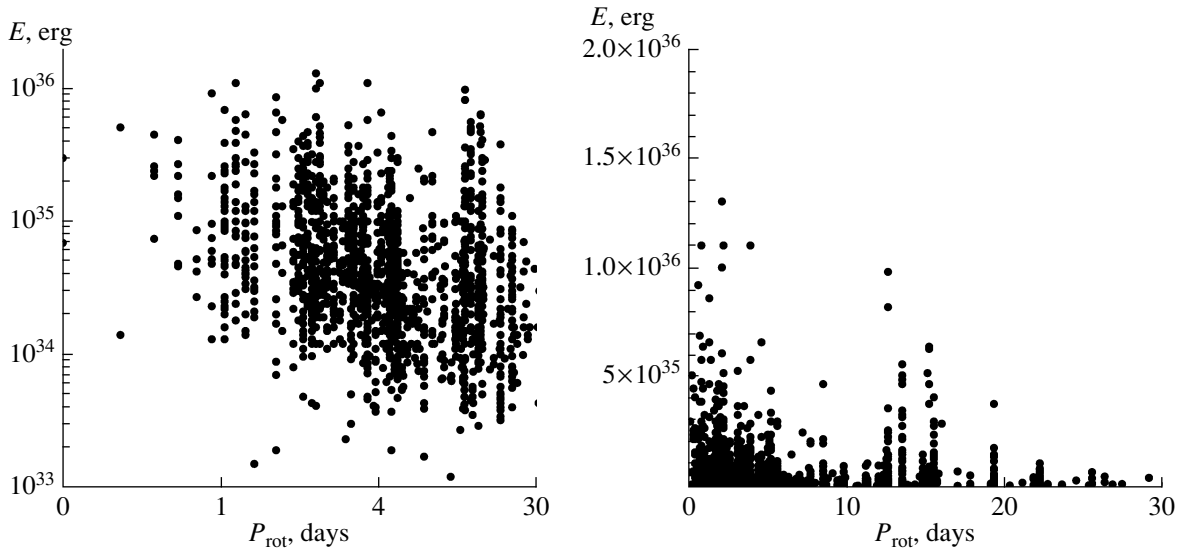

Fig. 1. Right: dependence of the superflare energy E for objects from [4] on their rotational periods P. Left: the same dependence on a logarithmic scale (see text).

rotation $\Delta\Omega$. The spottedness parameter and $\Delta\Omega$ as functions of the Rossby number and the superflare energy were compared, and a diagram plotting the superflare energy vs. the inverse of the Rossby number was constructed. Our preliminary analysis showed that none of these comparisons (for a sample of objects common to [4] and [5]) provided evidence for the presence of obvious regularities. Results for five stars for which several dozen flares were registered in [4] were also analyzed in [3].

Comparison of the spottedness parameter S and the superflare energy E did not reveal any obvious dependence between these parameters. It was found that substantial variations in the energy could be observed for small variations in S for a single star. Moreover, analysis of the star KIC 10422252 established that the parameter S can increase by a factor of six, while the flare energy can vary by an order of magnitude for any value of S.

We have carried out additional analyses of diagrams relating the superflare energy and parameters of the stellar activity (the area of the magnetic spots), and also carried out a more extensive analysis for stars for which several dozen flares were registered in [4]. Two such objects with an enhanced superflare rate—KIC 11551430 and KIC 11764567—are analyzed in detail.

2. ACTIVE REGIONS AND SUPERFLARE ENERGY

Our calculations of the spottedness S were used in [3] to carry out a number of additional comparisons of the parameters of stars displaying superflares. The comparisons in [3] for objects from [4] did not provide evidence for the presence of any clearly manifest relations between the parameters considered (e.g., dependences of the spottedness S and $\Delta\Omega$ on the Rossby number ($\mathrm{Ro} = P_{\mathrm{rot}})/\tau_c$, where P_{rot} is the rotational period, and the duration of a convective turn, τ_c, or the inverse of the Rossby number).

Let us return to a more detailed analysis of the characteristics of stars with superflares. As a rule, the above dependences can conveniently be considered using diagrams plotting one parameter against another on a logarithmic scale (see, e.g., the plot in the left-hand panel of Fig. 1, which presents the dependence of the superflare energies for objects from [4] on their rotational periods). Shibayama et al. [4] conclude that the maximum flare energies for the stars considered do not depend on their rotational periods P. However, this conclusion must be confirmed based on the accumulation of new data capable of refining the statistical properties of the superflares. The origin of the lower envelope for the majority of points on this diagram seems to indicate the presence of a negative correlation, but Shibayama et al. [4] suggest that this instead reflects observational limitations on their method for detecting superflares. In this case, these results admit another interpretation, namely, that the entire range of superflare energies (right up to two orders of magnitude) can be reached by stars with virtually the entire range of rotational periods.

Another possibility arises from the version of this diagram constructed on a non-logarithmic scale (the right-hand panel in Fig. 1): the possible presence

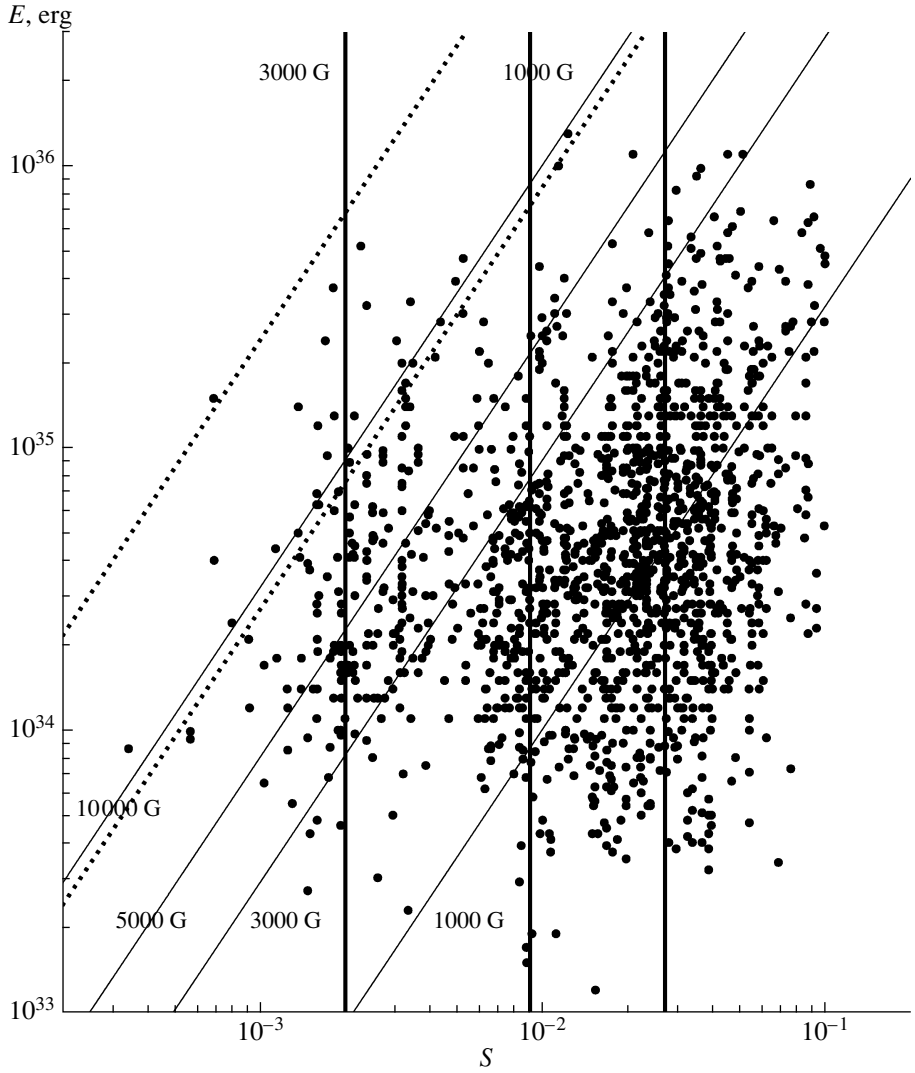

Fig. 2. Comparison of the superflare energy E with the spotted area S. The vertical lines separate three groups of objects (from right to left): stars with spots occupy 1−1.1% of the visible area of the star (the most numerous group), stars with $S \simeq 0.9\%$, and stars with $S \simeq 0.1\%$. The inclined lines show analytical dependences relating the flare energy with the area of cool spots for four magnetic fields $B = 1000$, 3000, 5000, and 10 000 G. The analytical dependences were calculated for two angles between the rotational axis of the star and the line of sight: $i = 90^\circ$ and $i = 3^\circ$ (solid and dotted lines, respectively).

of a bimodal distribution with a dip for objects with $P \approx 10$ days. There are relatively few data for objects with periods exceeding 10 days, making it difficult to determine whether the maximum flare energies for the different groups are the same (we might expect that more rapidly rotating stars should have flares with higher energies?).

Figure 2 presents the results of comparing the superflare energy with the areas of cool spots detected quasi-simultaneously (during the corresponding axial rotation of the star [4]) calculated by us in [6]. Our diagram is analogous to Fig. 10 of [7]; however, we note that the spot areas in [7] were calculated using a very approximate relation that systematically differs from the more precise model computations of [6], which prompted us to repeat this analysis. It would be natural to suppose the presence of a dependence of the flare energy on S (i.e., high flare energies could be explained as high magnetic energies accumulated in more spotted stars). However, if such a dependence exists, it is expressed very weakly. Further, in our opinion, there is evidence for the existence of three groups of objects: stars with spotted areas S exceeding 1−1.1% of the visible surface of the star (the most numerous group), stars with $S \simeq 0.9\%$, and stars with $S \simeq 0.1\%$. The range of flare energies within each of these three groups is approximately the same. Figure 2 presents analytical dependences

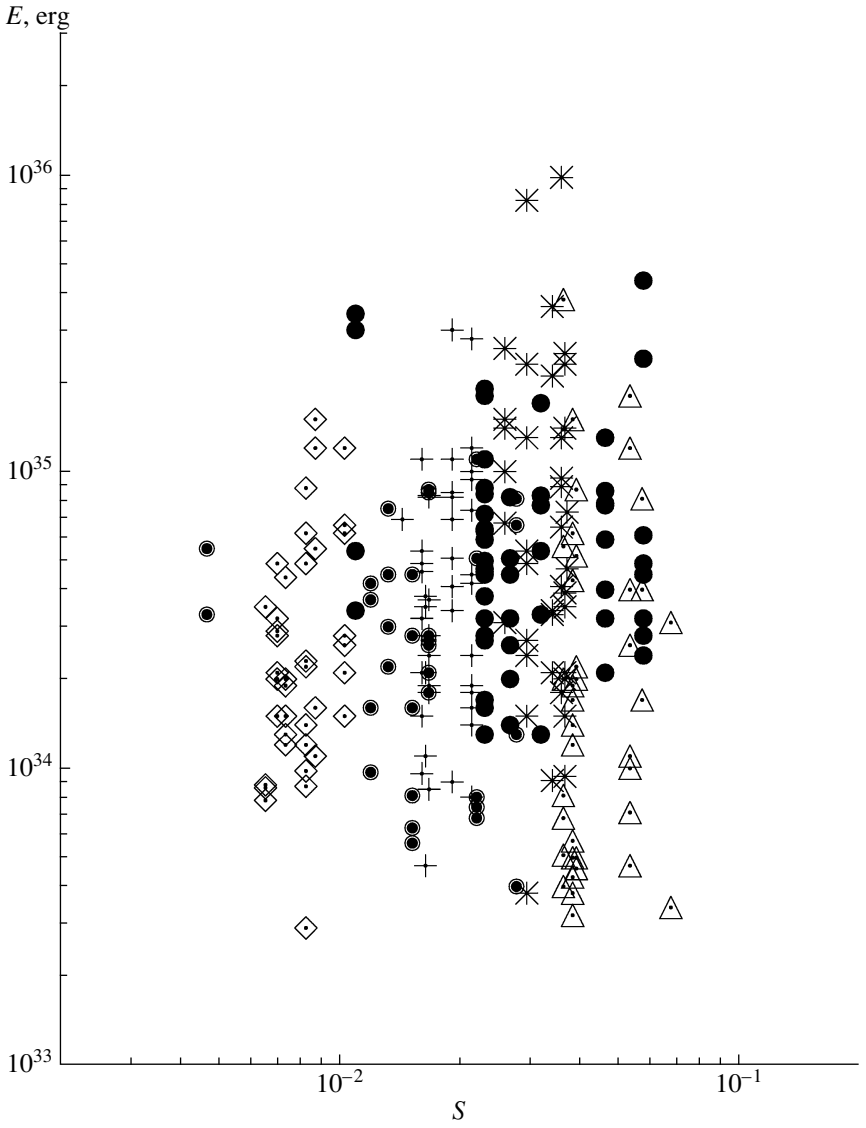

Fig. 3. Comparison of the superflare energy E and the spottedness parameter S for several stars from the sample [4], including objects with more than 20 superflares. The data for different stars are shown by different symbols; the filled circles show the data for KIC 10422252 and the encircled filled circles the data for KIC 11764567 (see the text).

between the superflare energy and the spotted area for the four magnetic fields $B = 1000$, 3000, 5000, and 10 000 G [7, formula (14)]. The analytical dependences were calculated for two inclinations i between the rotational axis of the star and the line of sight (90° and 3°).

Analysis of the data in Fig. 2 confirms and refines the earlier conclusions of [7]. The majority of points lie to the right of the dependence corresponding to $B = 3000$ G for $i = 90°$ (these points form the first two groups of objects we have distinguished). Due to differences in the calculated S values (our values and those in [7]), this same conclusion can be drawn for the data in [7] for $B = 1000$ G. We can explain the positions of stars in the third group in this diagram (i.e., to the left of the dependence for $B = 3000$ G and $i = 90°$) in several ways. Most importantly, it is obvious that the angle i (which we have not estimated for the objects considered) will not be equal to 90° for all the objects, and can vary in the range 0°–90°. Moreover, Notsu et al. [7] suggest that the magnetic field is not constant, and could be a function, for example, of the spottedness, making the dependence more complex than is presented in Fig. 2.

The vast majority of points in Fig. 2 lie to the right of the dependence for $B = 1000$ G and $i = 3°$. Following Notsu et al. [7], this fact can be interpreted

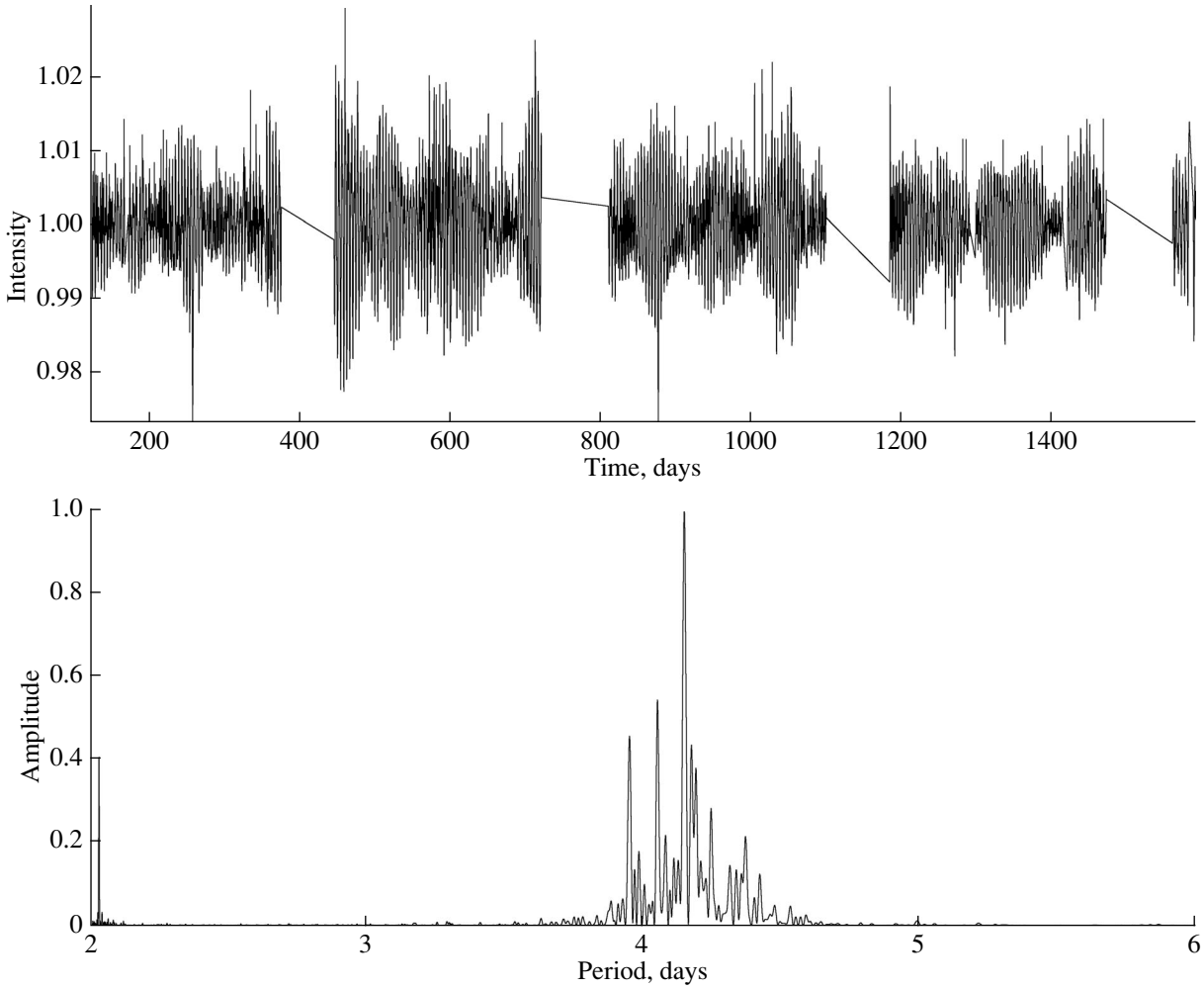

Fig. 4. Upper: light curve of KIC 11551430 from data obtained from the Kepler Space Telescope archive. Lower: power spectrum for the period range 2–6 d.

as evidence that the flare activity is not directly related to circumpolar active regions.

An analysis of the data of [4] is of special interest, since they enable a direct comparison of the flare energy and the simultaneously measured spottedness S. Figure 3 presents a comparison of S with the energies of superflares E for several stars from the sample, including objects displaying more than 20 superflares. As we found earlier in [3], the same star can display substantial variations in energy for small variations in S (the flares can vary by up to two orders of magnitude with virtually identical areas of magnetic spots). It is especially striking that substantial variations in spottedness (by factors of five to six) were detected for only two objets in the entire sample (KIC 10422252 and KIC 11764567). At the same time, flare energy variations of orders of magnitude can be reached for any level of spottedness.

3. ANALYSIS OF THE ACTIVITY OF KIC 11551430 AND KIC 11764567

Detailed studies of solar-type stars with superflares (including spectroscopic studies [8]) are only beginning. Here, we present the results of a detailed analysis of the activity of the two stars KIC 11551430 and KIC 11764567 based on all available photometric data from the Kepler Space Telescope archive. We chose these objects for two reasons. KIC 11551430 displayed the highest number of flares in [9], namely, 202. KIC 11764567 was chosen as the slowly rotating star ($P > 10$ d) displaying the highest number of flares (59). Stars of this type are of special interest from the point of view of predicting the possibility of superflares on the Sun.

The data reduction was analogous to that carried out earlier in [10,11]. We used the latest version of the instrumental corrections to the light curves available

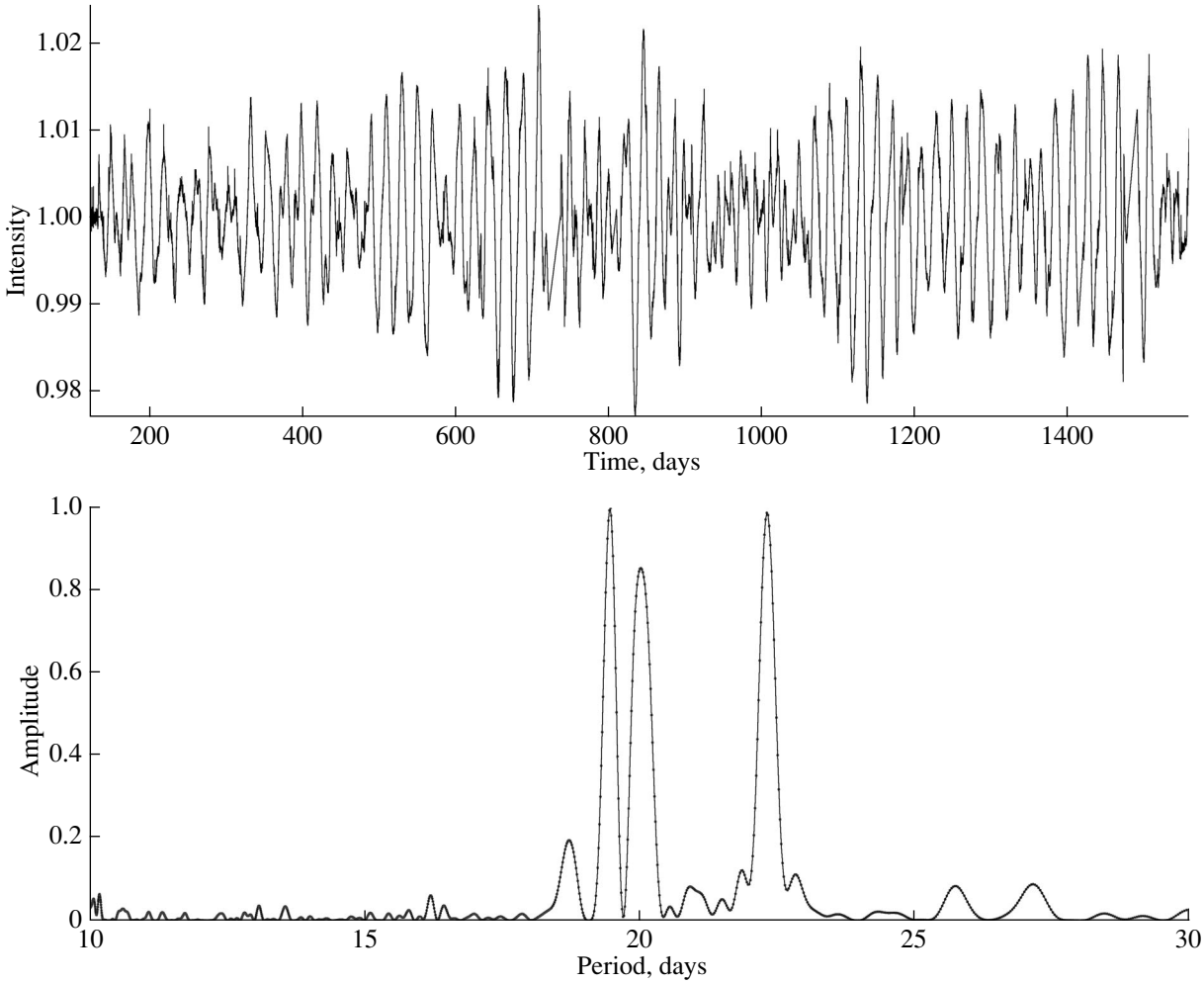

Fig. 5. Upper: light curve for KIC 11764567 from data obtained from the Kepler Space Telescope archive. Lower: power spectrum for the period range 10–30 d.

in the archive. We selected 50 728 and 63 560 individual brightness measurements for KIC 11551430 and KIC 11764567, respectively, for our analysis, obtained during an interval of nearly four years. The calculated power spectra (Figs. 4 and 5) indicate fairly complex brightness variability of the two stars, and consequently a complex character for variations in their activity. The power spectra show a number of peaks with various amplitudes whose origin could be associated with the presence of spots (or groups of spots) located at different latitudes on the differentially rotating stars (as was suggested by us earlier in [12, 13]). Variations in the brightness-variability periods could correspond to variations in and evolution of the active regions lying at various latitudes on the stellar surface. We analyzed the photometric variability of the stars further using their "mean photometric" periods, equal to 4.15 and 19.7 d for KIC 11551430 and KIC 11764567, respectively. We applied a similar approach earlier when analyzing the activity of the star HD 199178 [14] and the K dwarf KIC 8429280 (TYC 3146-35-1) [15].

Our earlier publications (see [14, 15]) contain a detailed description of the analysis of light curves (including those ofbtained with the Kepler Space Telescope) using the iPH program [16]. We took the parameters of the stellar atmospheres from [9], and used data from the grid of model atospheres of Kurucz in the computations. We determined the longitudes corresponding to the maximum filling factors f from the resulting maps of the surface temperature inhomogeneities. In most cases, the spots are concentrated at two longitudes, expressed as two independent active regions. There were almost always two active regions on the surfaces of the studied stars (Fig. 6 for KIC 11764567). The distance in longitude between these two regions was constant for KIC 11764567, and equal to about 0.5 in phase. The distance be-

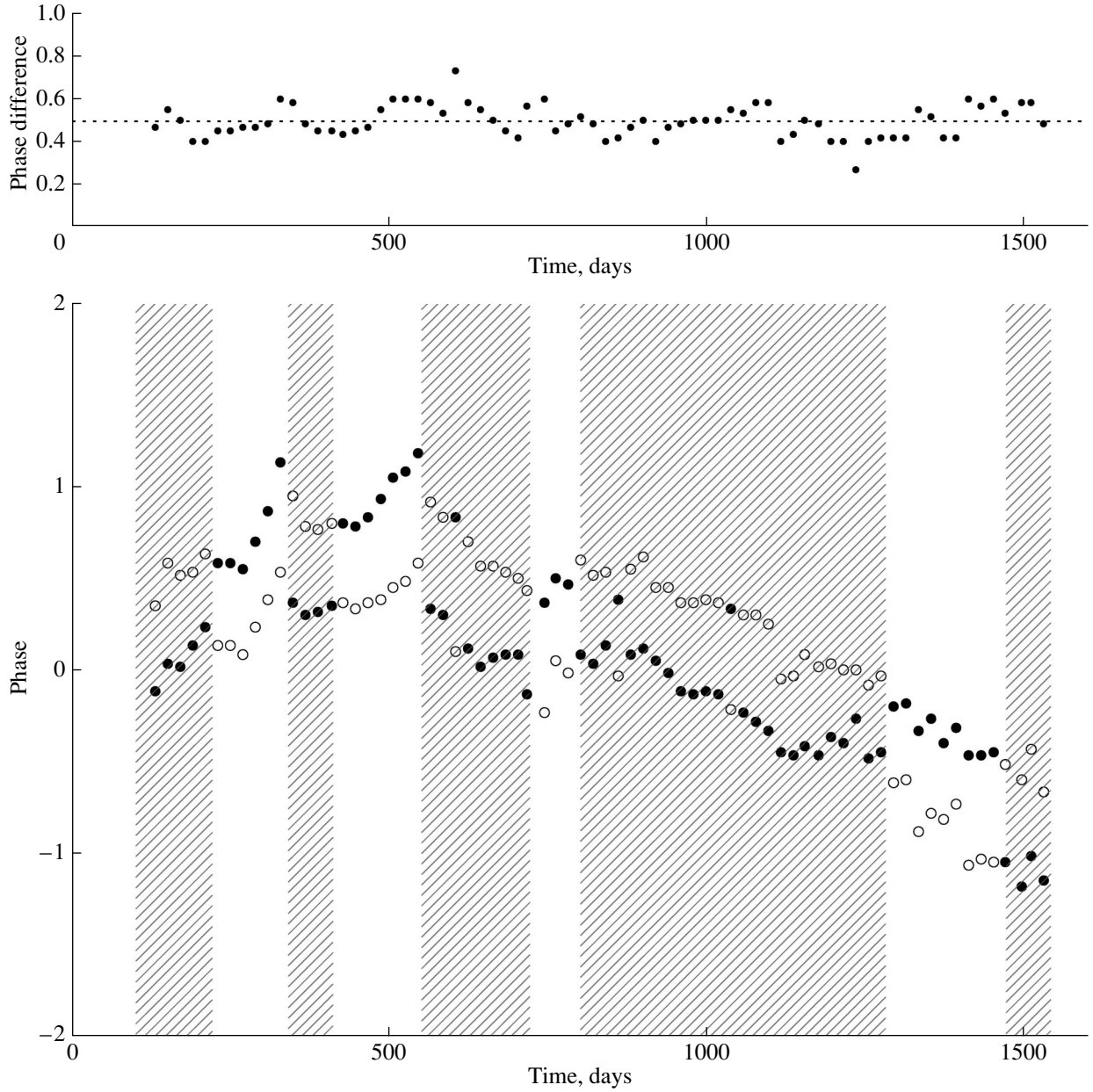

Fig. 6. Lower: phases of active regions on the surface of KIC 11764567; dark circles show more active and hollow circles less active regions. The shaded and unshaded regions denote time intervals corresponding to various positions of the active regions. Upper: distance (in phase) between active regions (see the text).

tween the active longitudes of KIC 11551430 was not constant, and varied from 0.4 to 0.6 in phase, with the mean phase close to 0.5.

The systematic shift of the positions of the active longitudes (e.g., Fig. 6 for KIC 11764567) is due to our use of the mean photometric period. By the end of the observations, the position of the less active region on the surface of KIC 11764567 had large uncertainties. Multiple exchanges in the longitudes of the active regions on the stellar surface occurred during the observing interval. The duration of the intervals between these exchanges varies from tens to several hundred days. The spottednesses of KIC 11551430 and KIC 11764567 were 2.5 and 3%, respectively, of the area of the total visible surfaces of these objects.

4. CONCLUSION

We have carried out additional analyses of diagrams plotting the energy of superflares against parameters of the stellar activity (the area of their

magnetic spots), and also conducted more extensive studies of the activity of two stars with the highest numbers of superflares [4]. With this aim, we analyzed the properties of the active regions (cool spots) on the surfaces of 279 G stars, between them displaying more than 1500 superflares with energies of 10^{33}–10^{36} erg. Our calculations of the spottedness parameter S and $\Delta\Omega$ [6] made it possible to broaden consideration of various comparisions of the parameters of stars exhibiting superflares.

Our results have led us to the following conclusions.

1. We have supplemented the conclusion of [4] that the maximum energy of superflares is independent of the stellar rotational periods P with the suggestion that the entire range of variations of the flare energies is independent of P.

2. We have proposed that the logarithmic plot of the superflare energy vs. the stellar rotational period is bimodal, and suggested that two groups of objects without very different maximum superflare energies can be distinguished—those with rotational periods greater than and less than 10 d.

3. Analysis of the diagrams displaying comparisons of the superflare energy and the area occupied by cool spots suggests the possible existence of three groups of objects: stars whose spotted areas S exceed 1–1.1% of the visible area of the star (the most numerous group), stars for which $S \simeq 0.9\%$, and stars for which $S \simeq 0.1\%$. The range of variations of the flare energy are roughly the same for each of these three groups.

4. The majority of points on this diagram lie to the right of the dependence corresponding to $B = 3000$ G and $i = 90°$ (the first two groups of objects). The location of the third group of objects to the left of the dependence for $B = 3000$ G and $i = 90°$ could be due, for example, to the fact that the angle i is not equal to 90° for all the objects, as well as the fact that, according to [7], the magnetic field may not be constant, and could be a function of the size of the spots and other factors.

5. Based on our new, more precise determinations of the parameter S [6], we have confirmed the conclusion of [7] that the flare activity is not directly related to circumpolar active regions, since the vast majority of points in Fig. 2 lie to the right of the dependence for $B = 1000$ G and $i = 3°$ (the stars are essentially viewed pole-on).

6. Our analysis of stars from a sample including objects with more than 20 superflares has shown that substantial variations in the flare energy can be achieved in the presence of only small variations in S for a single star (the range of flare energy can reach two orders of magnitude with essentially the same area occupied by magnetic spots). Only two objects in the sample displayed substantial variations in their spottedness (by factors of five to six; KIC 10422252 and KIC 11764567). Variations in the flare energy by orders of magnitude were observed for any level of spottedness.

7. All available measurements from the Kepler Space Telescope archive were used to carry out a detailed analysis of the activity of KIC 11551430 and KIC 11764567. Our interest in these two objects is due to the fact that KIC 11551430 displayed the highest number of flares (on average, one flare every seven days!), while KIC 11764567 displayed the highest number of flares among stars with rotational periods comparable to the solar value (on average, one flare every 25 days). The power spectra for the data characterizing the brightness of these objects contain a number of peaks with various amplitudes (which we suggest are due to the presence of groups of spots located at different latitudes on the surfaces of the differentially rotating stars). The results of computations with the iPH program were used to construct maps of the surface temperature inhomogeneities for the studied stars, and determine the longitudes corresponding to the locations of active regions. There were almost always two active regions present on the stellar surfaces. The distance between the active regions was essentially constant for KIC 11764567 (0.5 in phase), while this distance ranged from 0.4 to 0.6 in phase for KIC 11551430. There were multiple exchanges in the longitudes of the active regions on the stellar surfaces. The duration of the intervals between exchanges ranged from tens of days to four hundred days. The surface spottednesses of KIC 11551430 and KIC 11764567 were, on average, 2.5 and 3% of the areas of their total visible surfaces, respectively.

ACKNOWLEDGMENTS

We thank the Kepler Space Telescope archive and MAST (the archive of B.A. Mikulski for space-telescope data) teams for the possibility of using the corresponding observational data. This work was supported by the Basic Research Program of the Presidium of the Russian Academy of Sciences "Transitional and Explosive Processes in Astrophysics" (P-41).

REFERENCES

1. H. Maehara, T. Shibayama, S. Notsu, Yu. Notsu, T. Nagao, S. Kusaba, S. Honda, D. Nogami, and K. Shibata, Nature **485**, 478 (2012).
2. B. T. Tsurutani, W. D. Gonzales, G. S. Lakhina, and S. Alex, J. Geophys. Res. **108**, 1268 (2003).
3. I. S. Savanov, Astrophys. Bull. **70**, 83 (2015).

4. T. Shibayama, H. Maehara, S. Notsu, Yu. Notsu, T. Nagao, S. Honda, T. T. Ishii, D. Nogami, and K. Shibata, Astrophys. J. Suppl. Ser. **209**, 5 (2013).
5. T. Reinhold, A. Reiners, and G. Basri, Astron. Astrophys. **560**, A4 (2013).
6. I.S. Savanov, Astrofiz. Byull. (2015, in press).
7. Y. Notsu, T. Shibayama, H. Maehara, Sh. Notsu, T. Nagao, S. Honda, T. T. Ishii, D. Nogami, and K. Shibata, Astrophys. J. **771**, 127 (2013).
8. R. Wichmann, B. Fuhrmeister, U. Wolter, and E. Nagel, Astron. Astrophys. **567**, 36 (2014).
9. Ch.-J. Wu, W.-H. Ip, and L.-Ch. Huang, Astrophys. J. **798**, 92 (2015).
10. I. S. Savanov, Astron. Rep. **55**, 341 (2011).
11. I. S. Savanov, Astron. Rep. **56**, 716 (2012).
12. I. S. Savanov and E. S. Dmitrienko, Astron. Rep. **57**, 757 (2013).
13. I. S. Savanov and E. S. Dmitrienko, Astron. Rep. **56**, 116 (2012).
14. I. S. Savanov, Astron. Rep. **53**, 1032 (2009).
15. I. S. Savanov, Astron. Rep. **55**, 801 (2011).
16. I. S. Savanov and K. G. Strassmeier, Astron. Nachr. **329**, 364 (2008).

Translated by D. Gabuzda